Data-driven methodology to detect and classify structural changes under temperature variations

2014 Smart Mater. Struct. 23 045006

(http://iopscience.iop.org/0964-1726/23/4/045006)

IOP Publishing

Smart Materials and Structures

Smart Mater. Struct. **23** (2014) 045006 (15pp)

doi:10.1088/0964-1726/23/4/045006

Data-driven methodology to detect and classify structural changes under temperature variations

Maribel Anaya[1], Diego A Tibaduiza[2], Miguel A Torres-Arredondo[3], Francesc Pozo[1], Magda Ruiz[1], Luis E Mujica[1], José Rodellar[4] and Claus-Peter Fritzen[5]

[1] CoDAlab, Departament de Matemàtica Aplicada III, Escola Universitària d'Enginyeria Tècnica Industrial de Barcelona (EUETIB), Universitat Politècnica de Catalunya-BarcelonaTech (UPC), Comte d'Urgell 187, E-08036 Barcelona, Spain
[2] MEM (Materials-Electronics and Modelling Research Group), Faculty of Electronics Engineering, Universidad Santo Tomás-Colombia, Cra 9 No. 51-11, Bogotá-Colombia, Colombia
[3] University of Siegen, Centre for Sensor Systems (ZESS), Siegen, Germany
[4] CoDAlab, Departament de Matemàtica Aplicada III, Escola Tècnica Superior d'Enginyers de Camins, Canals i Ports de Barcelona (ETSECCPB), Universitat Politècnica de Catalunya-BarcelonaTech (UPC), Jordi Girona 1-3, E-08034 Barcelona, Spain
[5] University of Siegen, Institute of Mechanics and Control Engineering-Mechatronics, Paul-Bonatz-Strasse 9-11, D-57076 Siegen, Germany

E-mail: maribel.anaya@upc.edu

Received 24 August 2013, revised 7 January 2014
Accepted for publication 10 January 2014
Published 28 February 2014

Abstract

This paper presents a methodology for the detection and classification of structural changes under different temperature scenarios using a statistical data-driven modelling approach by means of a distributed piezoelectric active sensor network at different actuation phases. An initial baseline pattern for each actuation phase for the healthy structure is built by applying multiway principal component analysis (MPCA) to wavelet approximation coefficients calculated using the discrete wavelet transform (DWT) from ultrasonic signals which are collected during several experiments. In addition, experiments are performed with the structure in different states (simulated damages), pre-processed and projected into the different baseline patterns for each actuator. Some of these projections and squared prediction errors (SPE) are used as input feature vectors to a self-organizing map (SOM), which is trained and validated in order to build a final pattern with the aim of providing an insight into the classified states. The methodology is tested using ultrasonic signals collected from an aluminium plate and a stiffened composite panel. Results show that all the simulated states are successfully classified no matter what the kind of damage or the temperature is in both structures.

Keywords: damage classification, damage index, discrete wavelet transform (DWT), principal component analysis (PCA), self-organizing maps (SOM), structural health monitoring (SHM), temperature effects

(Some figures may appear in colour only in the online journal)

1. Introduction

Structural health monitoring (SHM) is an important discipline that attempts to assess the proper performance of a structure. To achieve this objective, SHM systems make use of sensors permanently installed in the structure for inspecting and defining its current state based on the analysis of structural responses. As a result, the collected structural responses are analysed and compared with baseline patterns in order to detect abnormal characteristics and define the structural integrity. The obtained information can be used to decide whether the structure can operate under safe and reliable conditions.

In SHM different levels of damage diagnosis can be achieved [1]. In a general way, these can be grouped in four levels. The first level includes the damage detection and its main objective is to know whether there is any abnormality in the structure and if this abnormality corresponds to damage. The second level includes the damage localization and allows determining the position of the damage in the structure. The third step includes classification tasks to define the type of damage and its size. Finally, level 4 is focused on knowing the structure remaining lifetime. In general, the damage identification can be performed following two main approaches. The first approach consists in obtaining a reliable physics-based model of the structure, while the second is based on data-driven approaches that normally tackle the problem as one of pattern recognition. One advantage of the use of data-driven approaches is the reliability in the analysis since the indication of damage could be directly determined with a comparison between a baseline and the collected data. However, to ensure the reliability of the analysis performed to the collected signals in several experiments, it is necessary to consider variations in the environmental and operational conditions, and the proper functioning of the sensors, actuators and hardware that are used to inspect the structure.

Different kinds of damage can be found in the normal service of a structure and these depend on the material, its configuration, its specific use and the environmental and operational conditions among others. Some typical examples are cracks, debonding in sandwich structures, spalling of concrete cover, buckling of reinforced rods and delamination. In the same way, these kinds of damage can be produced by different mechanisms. The following categories can be distinguished.

- Gradual damage producing mechanism such as fatigue, corrosion and aging.
- Sudden and predictable damage producing mechanism coming from aircraft landing and planned explosions in confinement vessels.
- Sudden and unpredictable damage producing mechanism originating from foreign-object impact, earthquakes and wind loads.

At the same time, each type of damage can also be classified depending on their severity into three big groups [3].

- Light damage. This corresponds to the initial stage of damage, which can be relatively easily repairable and is not dangerous for the normal operation of the structure.
- Moderate damage. In comparison with the previous type, this damage requires major repairs and needs to be evaluated more carefully in order to define if the structure can operate in normal conditions.
- Severe damage. This type of damage, unlike the previous, requires major reparations or the replacement of the structure.

Success in damage identification depends not only on the methodology developed but also on the correct operation of sensors permanently attached to the structure. In this sense, as in all sensing systems, it is need to ensure that it operates properly. In the case of piezoelectric systems, debonding and sensor breakage are the big issues to consider. It is important to consider both types of failure in the detection tasks since false alarms can be detected by the SHM system without damage in the structure. The main problem of sensor debonding is that it cannot be detected by any visual inspection technique and it can appear because of loadings, degradation of the adhesive bond or impacts, among others. Sensor breakage is more common in impacts with foreign objects. It consists in a cut or cuts that reduce the total area of the sensor. More precisely, in the case of the piezoelectric transducers (PZTs) it has the effect of changing the signals applied and collected by the sensor [2, 38]. This paper considers sensor breakage problems; debonding problems will be considered in future works.

For a structure in service, the variability in its dynamic properties can be a result of time-varying environmental and operational conditions [4]. Some of the environmental conditions to consider are humidity, wind loads, temperature, altitude, radiation, vibrations and pressure. Operational conditions include loading conditions, operational speed and mass loading [4]. The design of methodologies to improve the damage identification including environmental and operational conditions is currently an area of active research interest. This interest is motivated by the fact that new designs in civil, aeronautics and astronautics include the use of more complex structures subjected to variable environmental and operational conditions. To assess the structural integrity it is necessary to have a reliable continuous monitoring that allows false alarms resulting from these variable conditions to be avoided. Since a structure in normal operating conditions undergoes temperature variations and different forces by the environmental conditions, it is necessary to understand the effects of such conditions and test the developed methodologies under these conditions.

This paper addresses levels one and three of the damage identification task by means of a methodology which uses a baseline with several data from different temperatures to classify structural states and fault sensor damage. As several works have shown, in metallic and composite materials the temperature influence is presented in the wave propagation. In fact, wave propagation is affected when the elastic properties and density of the propagation medium are shifted. In ultrasonic signals, changes in the temperature stretch or compress the signal and distort the shape [35–37]. These changes directly affect the performance of the methodologies and need to be considered. The methodology presented in this work considers

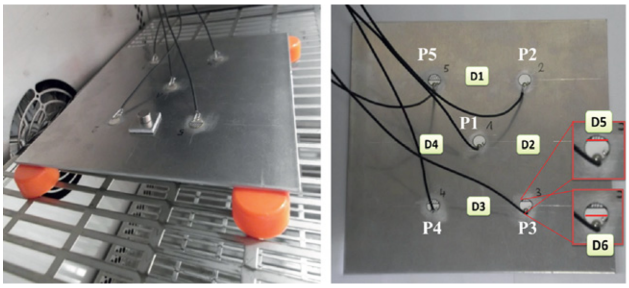

Figure 1. Aluminium plate and damage description.

Figure 2. Simplified aircraft composite skin panel: setup and damage positions.

the use of discrete wavelet transform (DWT), multiway principal component analysis (MPCA) and self-organizing maps (SOM) to solve the temperature change problem and it is tested using an aluminum plate instrumented with five piezoelectric transducers and a simplified aircraft composite skin panel which is instrumented with four piezoelectric transducers. On the one hand, seven different states are studied in the classification in the first structure: the undamaged state, four simulated damages (structural modifications by adding a mass at different positions of the structure) and two fault sensor (sensor breakage at 25% and 50%). On the other hand, six structural states are studied in the second structure: these states include the undamaged structure and five structural modifications that are simulated by means of adding a mass in different locations. The experimental results show that all these states are successfully detected and classified no matter what kind of damage or temperature in both structures.

The paper is organized as follows. Section 2 presents the experimental setup followed by the basic theoretical background on the concepts of discrete wavelet transform, PCA and self-organizing maps in section 3. The methodologies for the damage detection and classification are presented in section 4. The results of the application of the methodology to the different specimens are presented in section 5. Finally, conclusions are drawn in section 6.

2. Experimental setup

The validation of the methodology is carried out by using data collected from experiments performed on two different specimens. The first specimen corresponds to an aluminum plate with dimensions 200 mm × 200 mm which is instrumented with 5 PZT transducers (PIC-151) bonded on the surface as shown in figure 1. Six damages have been simulated on the structure. The first four damages are simulated by placing magnets on both sides of the structure at different positions. The other two damages correspond to a break or cut of the sensor patch to reduce the total area; 25% for damage 5 and 50% for damage 6. The location of the damages is shown in figure 1.

To inspect the structure, a 12 V Hanning windowed cosine train signal with five cycles and 50 kHz as the central frequency was used. This structure was subjected to temperature changes. To perform these experiments, the structure was placed in an oven with controlled temperature. Data from the structure under six different temperatures (24, 30, 35, 40, 45 and 50 °C) for each structural state were collected. To avoid the contact between the metallic surfaces and eliminate the noise in the experiments, plastic elements were used. 100 experiments were collected for each state and for each temperature.

The second structure is a simplified aircraft composite skin panel made of carbon fibre reinforced plastic (CFRP).The structure is depicted in figure 2. The overall size of the plate is approximately 500 mm × 500 mm × 1.9 mm and its weight is about 1.125 kg. The stringers are 36 mm high and 2.5 mm thick. The properties of the unidirectional (UD) material are $V_{\mathrm{Fibre}} = 60\%$, $E_1 = 142.6$ GPa, $E_2 = 9.65$ GPa, $\nu_{12} = 0.334$, $\nu_{13} = 0.328$, $\nu_{23} = 0.54$ and $G_{12} = G_{13} = 6.0$ GPa. The plate and the stringers consist of nine plies. All plies are aligned in the same direction. Damage on the tested composite plate was simulated by localized masses at different positions as in the previous case. Figure 2 outlines the coordinates for the simulated damage on the composite skin panel. The excitation voltage signal is a 12 V Hanning windowed cosine train signal with five cycles; 120 experiments were recorded per sensor–actuator configuration at five different temperatures (35, 45, 55, 65 and 75 °C). To determine the carrier central frequency for the actuation signal in each structure, a frequency sweep was performed and the spectral content of each signal was analysed. The carrier frequencies were found to be 50 kHz. The carrier frequency was chosen to maximize the propagation efficiency. This type of excitation generates a dominant A_0 mode that is propagated along the structure allowing a better interaction of the guided wave with the simulated damage.

3. Theoretical background

The damage detection and classification methodology presented in this work is based on the use of data-driven analysis. The analysis is performed by pre-processing the data collected from the structures using discrete wavelet transform and applying multiway principal component analysis and damage indices as pattern recognition techniques. Finally the results obtained in the statistical modelling with PCA and the damage indices are included in a classifier to perform the final analysis. As a classifier, self-organizing maps are used. Details of how these steps are applied will be explained in section 4. However,

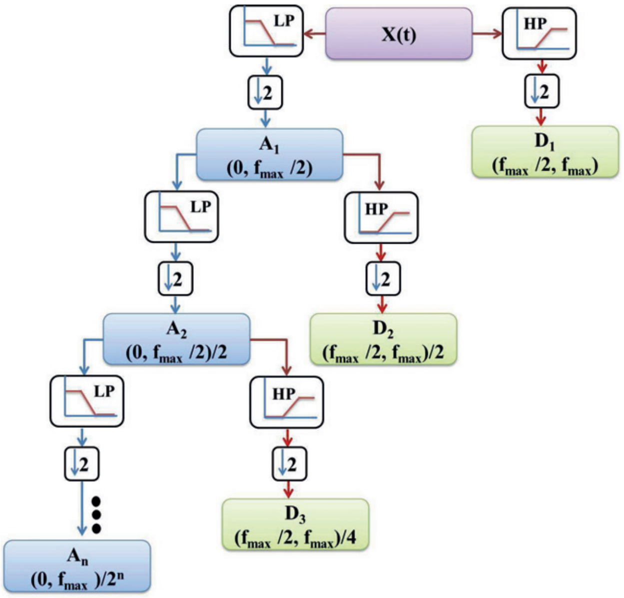

Figure 3. DWT decomposition tree.

a brief introduction to each method used in this methodology is included in this section. More details can be found in the references included in each method.

3.1. Discrete wavelet transform

The discrete wavelet transform (DWT) is a powerful tool specially used in areas dealing with the analysis of transient signals. This transform provides sufficient information for both the analysis and synthesis of the original signal with a significant reduction in the computational time cost compared with the analysis of the wavelet in the continuous time domain normally called the continuous wavelet transform (CWT) [14]. Roughly speaking, the characteristics of the given function at a specified time and scale are represented by the transformation coefficients. In other words, each wavelet coefficient represents time and frequency information of the signal. The DWT analysis can be performed by means of a fast, pyramidal algorithm related to a two-channel subband coding scheme using a special class of filter called quadrature mirror filters as proposed by Mallat [15]. In this algorithm, the signal is analysed at different frequency bands with different resolution by decomposing the signal into approximation and detail coefficients. This is achieved by successive high-pass (HP) and low-pass (LP) filtering of the input signal.

The optimum number of level decompositions could be determined, for example, based on a minimum-entropy decomposition algorithm [16]. Figure 3 shows the structure of the decomposition of the signal and the corresponding frequency bandwidths for the details ($\mathbf{D}_i$) and approximations ($\mathbf{A}_i$) [15]. Each level is obtained by the decomposition of the signal with high- and low-pass filtering and a downsampling of the input signal. The approximations represent the high-scale, low-frequency components of the signal. The details are the low-scale, high-frequency components. The frequency $\mathbf{f}_{\max}$ represents the maximum frequency contained in the recorded signal and n is the decomposition level. Discrete wavelets are often associated with dilation equations and scaling functions. The basic scaling function $\gamma(i)$ can be defined as

$$\gamma(i) = \sum_{m=0}^{j} c_m \gamma(2i - m), \tag{1}$$

where the values $c_m, m = 0, \ldots, j$ are the wavelet coefficients. These coefficients must satisfy certain conditions that are discussed in [18]. The scaling functions are then used to construct the corresponding wavelets $\phi(i)$ from the following formula:

$$\phi(i) = \sum_{m=0}^{j} (-1)^m c_m \gamma(2i + m - j + 1). \tag{2}$$

The approximation and detail coefficients can be calculated as follows:

$$A_{n,k} = 2^{-n/2} \sum_{i=1}^{j} x(i)\gamma(2^{-n} j - k), \tag{3}$$

$$D_{n,k} = 2^{-n/2} \sum_{i=1}^{j} x(i)\phi(2^{-n} j - k), \tag{4}$$

where γ is the scaling function, j is the number of discrete points of the input signal, and n and k are considered to be the scaling (dilation) index and the translation index, respectively. Each value of n allows analysis of a different resolution level of the input signal. Scaling functions are similar to wavelet functions except that they have only positive values and are designed to smooth the input signal [15, 17].

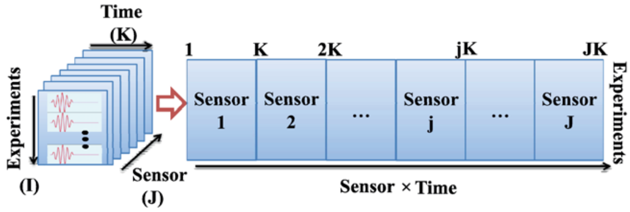

Figure 4. Unfolding the original data.

3.2. Multiway principal component analysis (MPCA)

MPCA is a very common practice in multivariate statistical procedures for monitoring the progress of batch processes [20, 21] and it is based on the fact that the data are inherently correlated [27]. This is similar to the use of PCA on a large two-dimensional matrix constructed by unfolding the three-way data matrix [26]. In this work the original data are expressed in a matrix whose dimensions are I experiments, K time instants and J sensors. This three-way data matrix is decomposed into a large two-dimensional matrix $\mathbf{X}$ as shown in figure 4.

3.3. Principal component analysis

Principal component analysis (PCA) is a useful technique of multivariable and megavariate analysis [6] that provides arguments to reduce a complex data set to a lower dimension and reveals some hidden and simplified structure/patterns that often underlie it. The goal of PCA is to discern which information is more important in the system by determining a new space (coordinates) to re-express the original data based on the variance–covariance structure. PCA can be also considered as a simple, non-parametric method for data compression and information extraction that finds combinations of variables or factors that describe major trends in a confusing data set. In order to develop a PCA model, it is necessary to arrange the collected data in a matrix $\mathbf{X}$. This $n \times m$ matrix contains information from m sensors and n experiments [7]. Since physical variables and sensors have different magnitudes and scales, each data-point is scaled using the mean and the standard deviation of all measurements of the sensor at the same time and the standard deviation of all measurements of the sensor. Once the variables are scaled, the covariance matrix $\mathbf{C}_\mathrm{x}$ is calculated as follows:

$$\mathbf{C}_\mathrm{x} = \frac{1}{n-1}\mathbf{X}^\mathrm{T}\mathbf{X}. \tag{5}$$

This is a square symmetric $m \times m$ matrix that measures the degree of linear relationship within the data set between all possible pairs of variables (sensors). The subspaces in PCA are defined by the eigenvectors and eigenvalues of the covariance matrix as follows:

$$\mathbf{C}_\mathrm{x}\tilde{\mathbf{P}} = \tilde{\mathbf{P}}\Lambda, \tag{6}$$

where the eigenvectors of $\mathbf{C}_\mathrm{x}$ are the columns of $\tilde{\mathbf{P}}$, and the eigenvalues are the diagonal terms of Λ (the off-diagonal terms are zero). Columns of matrix $\tilde{\mathbf{P}}$ are sorted according to the eigenvalues by descending order and they are called *principal components* of the data set or loading vectors. The eigenvectors with the highest eigenvalue represent the most important pattern in the data with the largest quantity of information. Choosing only a reduced number $r < m$ of principal components, those corresponding to the largest eigenvalues, the reduced transformation matrix could be imagined as a model for the structure. In this way, the new matrix $\mathbf{P}$ ($\tilde{\mathbf{P}}$ sorted and reduced) can be called a PCA model. Geometrically, the transformed data matrix $\mathbf{T}$ (score matrix) represents the projection of the original data over the direction of the principal components $\mathbf{P}$:

$$\mathbf{T} = \mathbf{X}\mathbf{P}. \tag{7}$$

In the full dimension case (using $\tilde{\mathbf{P}}$), this projection is invertible (since $\tilde{\mathbf{P}}\tilde{\mathbf{P}}^\mathrm{T} = \mathbf{I}$) and the original data can be recovered as $\mathbf{X} = \mathbf{T}\tilde{\mathbf{P}}^\mathbf{T}$. In the reduced case (using $\mathbf{P}$), with the given $\mathbf{T}$, it is not possible to fully recover $\mathbf{X}$, but $\mathbf{T}$ can be projected back onto the original m-dimensional space and one obtains another data matrix as follows:

$$\hat{\mathbf{X}} = \mathbf{T}\mathbf{P}^\mathrm{T} = (\mathbf{X}\mathbf{P})\mathbf{P}^\mathrm{T}. \tag{8}$$

The residual data matrix (the error when not all the principal components are used) can be defined as the difference between the original data and the projected back:

$$\mathbf{E} = \mathbf{X} - \hat{\mathbf{X}} = \mathbf{X}(\mathbf{I} - \mathbf{P}\mathbf{P}^\mathrm{T}). \tag{9}$$

In this paper, a comparison between the dynamical responses of the structure to be diagnosed and a baseline (pattern) allows one to determine if some changes exist on the structure and, besides, whether these changes can be considered as a damage or not. Transforming or projecting data from different states of the structure by using PCA would permit an easy and sometimes visual comparison between them. In some other cases, these projections are not sufficient and the use of some statistical measurements that can be considered as damage indices is necessary. There are several kinds of index that can give information about the accuracy of the model and/or the adjustment of each experiment to the model. In a general way, it is possible to define any index in the form

$$\mathbf{Index} = \mathbf{x}^\mathrm{T}\mathbf{M}\mathbf{x}, \tag{10}$$

where the column vector $\mathbf{x}$ represents measurements from all sensors at a specific experimental trial. Matrix $\mathbf{M}$ is a $m \times m$ squared matrix and depends on the type of index. Two well-known indices are commonly used to this aim: the *SPE-index* (or *Q-statistic*), where SPE stands for square prediction error and the Hotelling's T^2-*statistic* (also known as *D-index*) [7–10]. The former is based on analysing the residual data matrix to represent the variability of the data projection within the residual subspace. Denoting e_i as the i-th row of the matrix $\mathbf{E}$ (see equation (9)), the *Q-statistic* for each experiment can be defined as its squared norm as follows:

$$Q_i = \mathbf{x}_i^\mathrm{T}(\mathbf{I} - \mathbf{P}\mathbf{P}^\mathrm{T})\mathbf{x}_i. \tag{11}$$

In a previous work by the authors [19], it was demonstrated that in the methodology the use of the SPE-index and the scores allow a good classification, since the T^2-*statistic* is a measure calculated from the scores, and its use in the methodology in combination with the scores introduces redundancies to the analysis.

3.4. Self-organizing map (SOM)

The self-organizing map (SOM) is a kind of unsupervised neural network also known as a Kohonen network [11] in honour of the professor Teuvo Kohonen. This neuronal network is specialized in visualization and analysis of high-dimensional data and has the special property of generating one organized map in the output based on the inputs, grouping input data with similar characteristics in clusters [12, 34]. To do that, the SOM internally organizes the data based on features and their abstractions from input data. In particular, these maps have been used in practical speech recognition [30], robotics [29], control [31] and telecommunications [31], among others [13].

The structure of the SOM is a single feed forward network and each node in the input layer is connected to all the output neurons [28]. The connection between the input layer and the output layer is defined by a weighting matrix as shown in figure 5. In general, the inputs to the network are defined in the input layer and a weighting matrix relates each input with each cluster in the output layer.

The result of the SOM is an organized map which contains the final clustering of the input data. This information can be visualized by using the cluster map. The distance matrix techniques are widely used in the visualization of the

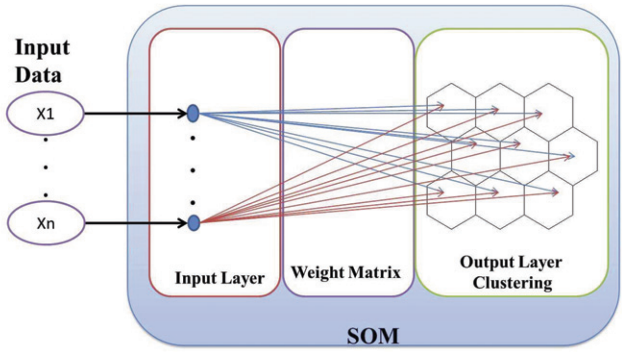

Figure 5. The self-organized map.

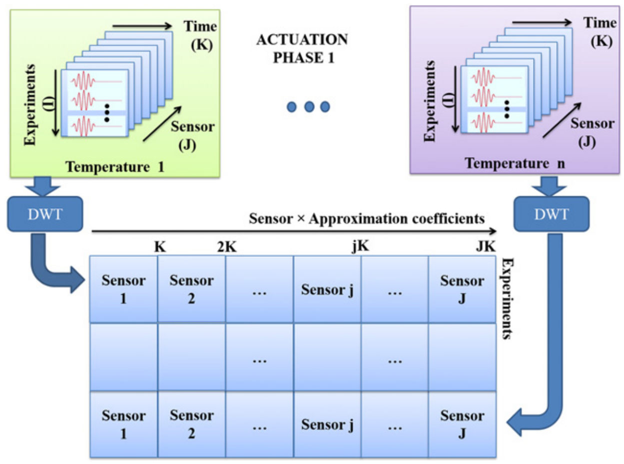

Figure 6. Unfolding the collected data in the actuation phase 1 using n temperatures.

cluster structure of the SOM. One of these techniques is the unified distance matrix, called U-matrix, which shows the separation between prototype vectors and neighbouring map units. The U-matrix is related to the linkage measure and can be visualized using a colour scale [32].

4. Damage detection and classification

In this paper, a methodology is proposed for damage detection and classification which is partly based on a methodology previously developed by the authors [3, 19, 33]. This methodology is considered to be used in plate-like structures instrumented with several sensors and uses ultrasonic signals to inspect the structure as a local approach. Further studies need to be considered to determine the application of this methodology in large-scale structures.

The proposed methodology considers the use of a multi-actuator piezoelectric system (distributed piezoelectric active network) working in several actuation phases, discrete wavelet transform, multiway principal component analysis (PCA), SPE-index and self-organizing maps for the classification of different structural states by considering temperature changes using robust baselines. In this case, a robust baseline is defined as a baseline with the data from the healthy structure at different temperatures. For building the baselines, the information about the temperature is not required because just the coefficients from the experiments at different temperatures are used to unfold the information by each actuation phase, as will be shown in the following paragraphs. The multi-actuator piezoelectric system consists of several piezoelectric transducers attached to the surface of the structure under test working in several actuation phases. In each actuation phase, one lead zirconium titanate (PZT) transducer is selected as actuator and a signal is applied to produce Lamb waves in the structure. On this paper the use of PZTs is considered since these can be easily attached to the surface of metallic structures and can work as sensors or as actuators. A study of the sensors to use needs to be considered in each particular application, because the piezoelectric sensors could not be useful in large civil applications where a large quantity of sensors is needed and the computational cost also needs to be considered for a successful application.

The signals propagated through the structure are collected in different points using the rest of the sensors and pre-processed by using the DWT. In this paper the DWT is used as a method for pre-processing the information by representing the high-dimensional original data from all the sensors attached to the structure to a compact representation by means of approximation coefficients. In this work the family of Daubechies wavelet basis function ‘db8’ was chosen for the methodology presented here since it proved to be adequate to encode and approximate the ultrasonic waveforms. This was accomplished by means of different trial-and-error tests by evaluating different mother wavelets and levels of decomposition so that the signal could be properly reconstructed from the calculated wavelet coefficients. The chosen ‘db8’ wavelet is an orthogonal wavelet with the advantage of avoiding phase shifts and allowing exact reconstruction of the signal. The index number refers to the number of coefficients. The number of vanishing moments for each wavelet is equal to half the number of coefficients, so the ‘db8’ has four vanishing moments. A vanishing moment confines the ability of the wavelet to represent polynomial behaviour [17, 23]. Special attention was paid to selection of the optimum decomposition level in order to avoid removing important information that could be related to some of the modes of propagation contained in the signal. The optimum number of level decompositions is determined based on both a minimum-entropy decomposition algorithm and systematic trials [16]. The entropy-based methods perform a systematic comparison of the signal and noise using the Shannon information theory [17]. It has been shown that a pure noise signal has the largest entropy while a systematic signal has zero entropy [24].

Figures 6–8 show the scheme of the methodology. In a first step, when working with one temperature, the dynamic responses collected from each actuator phase are stored by the data acquisition system in a matrix with dimensions $(I \times K)$, where I represents the number of experiments and K the number of sampling times. Denoting J as the number of PZT transducers that are receiving the dynamical responses for each experiment, J matrices with the information from each sensor by each actuator phase are finally stored. Therefore, the whole set of the data collected in each actuator phase and with a specific temperature can be organized in a three-dimensional

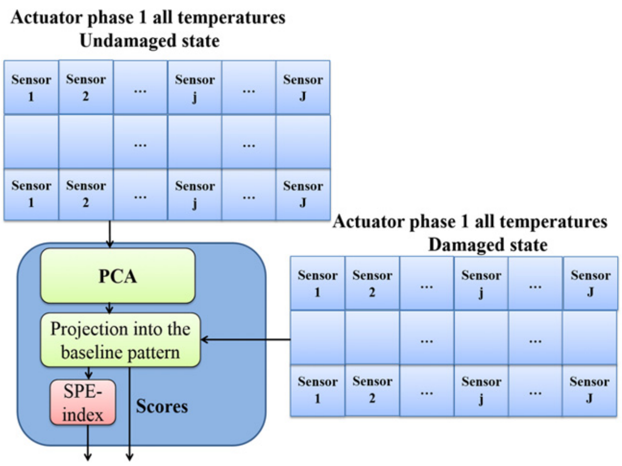

Figure 7. Calculation of the baseline pattern using PCA and calculation of scores and SPE-index in the actuator phase 1.

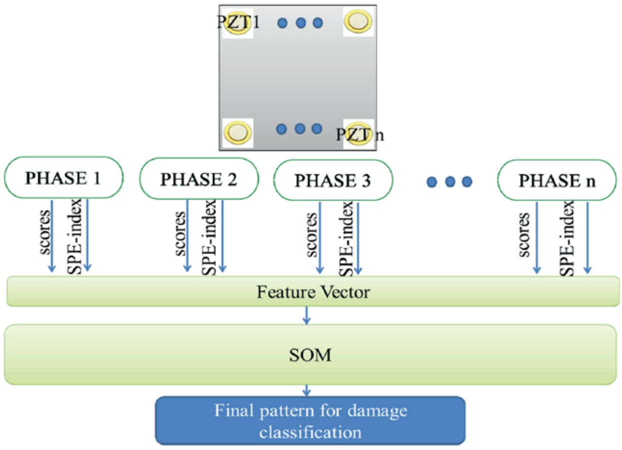

Figure 8. Final pattern for damage classification.

matrix $(I \times K \times J)$ or in a two-dimensional unfolded matrix $(I \times JK)$, where data from each sensor are located besides the other sensors as in figure 4. This is a very common practice in multivariate statistical procedures for monitoring the progress of batch processes [20, 21]. To manage the use of different temperatures, in this paper the data (approximation coefficient) from each temperature are unfolded and organized in a matrix as shown in figure 6 in order to obtain a matrix by each actuator phase with the information from all the sensors at different temperatures.

The collected data in each actuation phase must be pre-processed before the computation of the PCA model. For this kind of data sets (unfolded matrices), several ways of scaling have been presented in the literature: continuous scaling (CS), group scaling (GS) and auto-scaling (AS) [22]. According to these references, GS is selected for this work because this method considers changes between sensors and these sensors are not processed independently. Using this normalized data, a PCA model is built by each actuator phase. This way, the data are reduced by selecting a reduced number of components according to the cumulative percent variance (CPV) approach. The CPV approach guarantees the minimal model dimension that captures the desired variance. For the pre-processing step, the limitation is given by the processing capacity, since the data fusion implies the processing of a matrix with dimensions n (experiments) $\times\, md$ (sensors $\times$ approximation coefficients) by each actuation phase. As was previously mentioned, in the methodology data from a piezoelectric active system are considered. Even when in this paper it is not included, it would be interesting to test the proposed methodology with other types of sensor network, i.e. acceleration measurements, strain measurements, etc. However, this topic goes beyond the scope of the proposed paper and it would probably be evaluated in future work.

In a second step, the experiments are performed by evaluating the structure in the different possible states or scenarios (undamaged and with different kinds of damage) under different temperatures. The collected signals are pre-processed and organized in the same manner as in the first step. Afterwards, these signals are projected onto the corresponding PCA model (equation (7)), and the scores and the Q-index are obtained, as represented in figure 7.

With a predetermined number of scores and with the SPE-index, combining the results of all the actuator phases, a feature vector is built. This vector is used to apply data fusion and obtain a pattern with the information for the classification using all the structural states as shown in figure 8. This feature vector is then introduced as the input to a classifier. A SOM has been chosen as a classifier because its characteristics can provide good support for the classification and graphical representation, and group input data with similar features in clusters [19]. One important characteristic of this kind of ANN is that it does not need previous knowledge about the state of the structure (healthy or with some damage) to obtain the final clustering.

To visualize the results of the classification the U-matrix surface and the cluster map are used. The U-matrix surface allows the visualization of the distances between neurons by means of colours between adjacent neurons and the cluster map corresponds to another representation that can be used as a tool to show the different data set grouped with similar characteristics showing the clustering tendency. However, it is not possible to provide a multi-damage detection which is able to identify several damages occurring independently. Multi-damage scenarios will just be detected as an additional damage and generate an additional cluster in the SOM.

The proposed methodology is indeed a qualitative approach since a quantitative assessment of damage is not provided in the presented work.

5. Analysis and discussion of the results

5.1. Aluminum plate

The following three studies were conducted in order to verify and determine the approach sensitivity and the influence of the temperature variations in the detection and classification of damage.

(a) Classification of baselines at different temperatures.

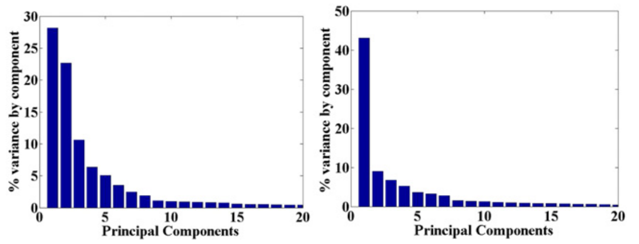

Figure 9. Percent of variance in the aluminum plate in (a) actuation phase 1 and (b) actuation phase 5.

(b) Damage detection and classification at each temperature level.
(c) Damage detection and classification using all temperatures.

5.1.1. Classification of baselines at different temperatures. Firstly, the classification of the different baselines at the different temperatures is evaluated. In particular, data from the structure at six different temperatures (24, 30, 35, 40, 45 and 50 °C) were used to evaluate the approach.

Following the scheme described in section 4, the wavelet approximation coefficients from the data of the healthy structure at different temperatures are computed. These approximation coefficients are organized as in figure 4 and then the baselines (PCA models) are built. To determine the number of principal components that will be used to project the new data, the variance captured by each principal component was computed for each temperature in order to determine the number of principal components. This analysis is fundamental in order to ensure that enough variance is captured by the model, therefore, allowing an optimal reduction. The distribution of the retained variance along the principal components in two of these actuator phases is depicted in figure 9. Only the components with a significant variance value are shown. The components with the highest variance represent variables or factors that describe major trends in a confusing data set. Similar results are obtained in the other actuation phases. From this analysis, the first 10 principal components are selected and used to define the PCA model by each actuator phase. This number of components considers more than 90% of variance in the statistical modelling.

New data from the structure to be diagnosed, in different states (healthy and damaged) are then collected and projected into the corresponding PCA model. These projections (scores) and the SPE-index are calculated by each actuation phase and used to define the feature vector and perform the data fusion as in the equation

$$F_i = \left[\text{score}_i^k \quad Q_i^k\right], \qquad (12)$$

where Score $= [\text{score}_1 \ldots \text{score}_n]$ with n principal components, k corresponds to the number of actuator phases and i is the number of experiments.

In order to define the optimal set of parameters to configure the map such as the normalization, the shape of the cluster map and its size, several SOMs are trained and validated.

Six possible normalizations are implemented in the toolbox to pre-process the input data: *range, var, log, logistic,*

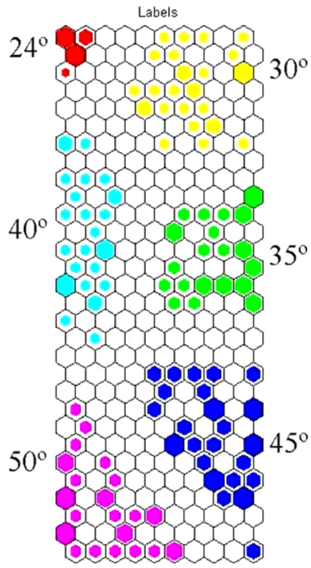

Figure 10. Classification of the different baselines at different temperatures using 10 scores and the SPE-index using the cluster map.

histD, histC [25]. According to [25], the normalization type *var*, performs a linear transformation which scales the value such that their variance is one. Normalization type *range* scales the variable values between [0,1] also using a linear transformation. *Log* normalization makes a logarithmic transformation of the input variables. The *logistic* normalization is more or less linear in the middle range and has a smooth nonlinearity at both ends, which ensures that all values (even in the future) are within the range [0,1]. Normalization type *histD* is a discrete histogram equalization. It sorts the values and replaces each value by its ordinal number. Finally, it scales the values such that they are between [0,1]. Normalization type *histC* is a continuous histogram equalization. The value range is divided into a number of bins and the values are linearly transformed in each bin. In a previous work by the authors [19], these normalizations were explored and the advantages and disadvantages of each normalization were explored. As a result, normalization type *histD* is selected on this work to normalize the feature vector. From this analysis a hexagonal lattice with a flat sheet shape is also defined. Different shapes such as sheet, cylinder or toroid can be chosen. For ease, a flat sheet shape is considered here. Finally, a cluster size of 30 × 10 is obtained to train the SOM.

The results of the training are presented by means of both the cluster map, in figure 10, and the U-matrix surface in figure 11. In the figures, the information about the temperature value is used just for labelling the results and the axis corresponds to the cluster size; in this sense, all the plots have 30 × 10 neurons. The analysis of these plots allows one to find differences between the data from the healthy structure at different temperatures. In this case six clusters seem to have been well identified in the cluster map and in the U-matrix surface. More precisely, the observations of the cluster map shows that the data from the structure when the temperature is 24 °C are better organized. This fact can be inferred by reviewing the number of output neurons occupied in the cluster

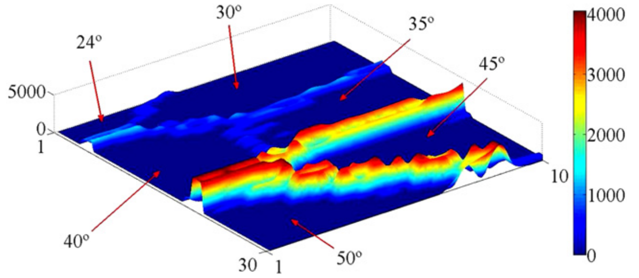

Figure 11. Classification of the different baselines at different temperatures using 10 scores and the SPE-index using the U-matrix surface.

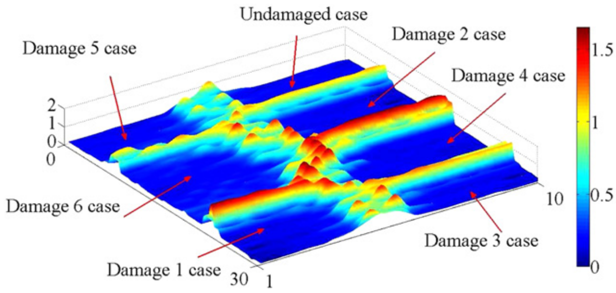

Figure 13. Classification of the different states at 24 °C using 10 scores and the SPE-index using the U-matrix surface.

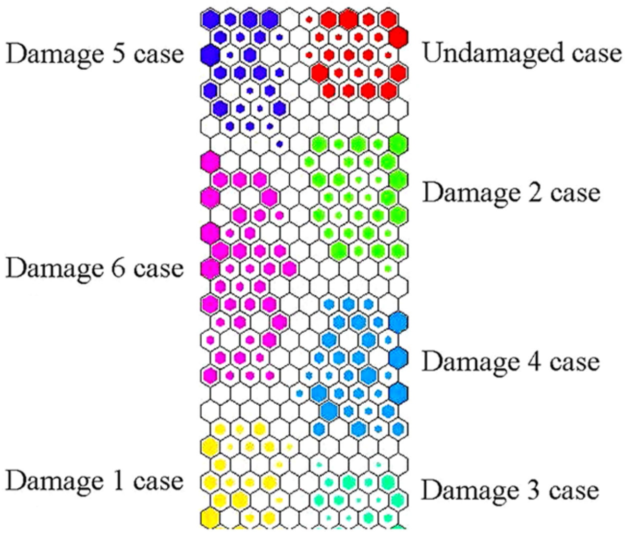

Figure 12. Classification of the different states at 24 °C using 10 scores and the SPE-index using the cluster map.

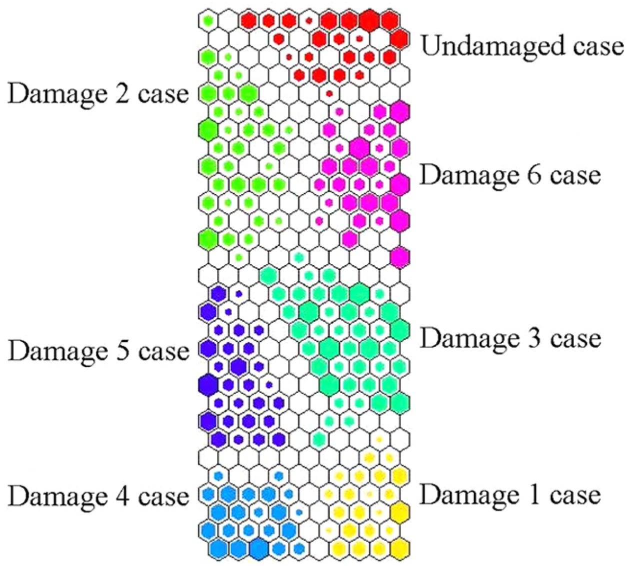

Figure 14. Classification of the different states at 40 °C using 10 scores and the SPE-index using the cluster map.

map. In the U-matrix surface the boundaries represent the separation between the clusters and the colour shows the magnitude of the differences between the clusters. In this sense, higher value colours according to the colour scale imply large separations. According to the colours at the boundaries, it can be seen that there are no significant differences between the first four temperatures. However, this difference is remarkable with respect to the last two temperatures. Another important issue is related to the management of the outliers. In the cluster map presented in figure 10, there is an outlier that corresponds to the structure at 45 °C. In this case, it is worth noting that the U-matrix surface (figure 11) allows the isolation of the outlier by the separation between the different areas. This separation represents the different zones delimited by boundaries, where the colours with low magnitude according to the colour scale depict these zones. The colours with high magnitude into these boundaries can be interpreted as the zones with a high separation between the clusters or the zones where the outliers appear. The result of this first study demonstrates the influence of the temperature despite the fact that the data comes from the healthy structure. These differences are not so evident with respect to the first temperatures.

5.1.2. Damage detection and classification by each temperature. In the second study, the maps were trained using the data from seven different states (healthy state and six damages). The normalization, the hexagonal lattice and the cluster size were defined as in the previous study. Four damages were simulated in the tested plate by adding a mass at different locations on the surface of the structure. In addition, two real damages in a sensor were performed. These damages correspond to a breakage at 25% and 50% of the sensor 3. Figures 12 to 17 show the classification results when the structure is exposed to a temperature of 24, 40 and 50 °C.

When the structure is exposed to a temperature of 24 °C, seven zones seem to have been well identified, as can be seen in figures 12 and 13. The boundaries between the clusters in the U-matrix surface show that there is a clear separation between all the states. Moreover, according to the cluster map there are no outliers.

Figures 14 and 15 show the results when the structure is exposed to a temperature of 40 °C. As it can be seen, there are seven clusters well identified in the cluster map and the U-matrix surface. As in the previous case, there is no presence of outliers. However, the damage distribution across the map is different.

The results when the structure is exposed to 50 °C (figures 16 and 17) show that all the states are clearly classified.

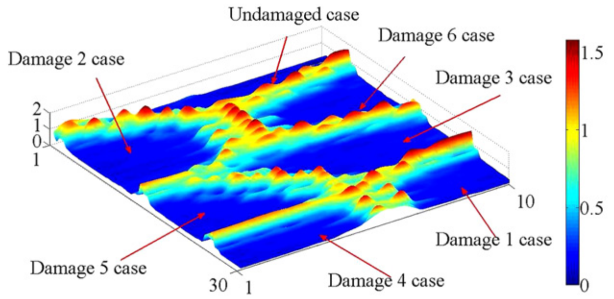

Figure 15. Classification of the different states at 40 °C using 10 scores and the SPE-index using the U-matrix surface.

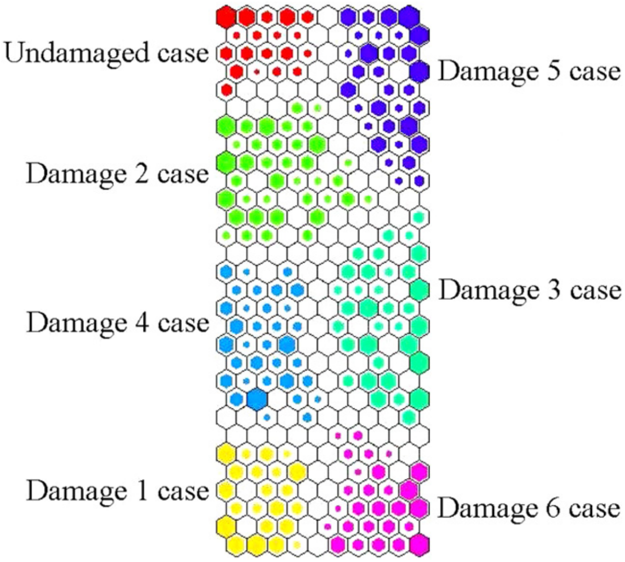

Figure 16. Classification of the different states at 50 °C using 10 scores and the SPE-index using the cluster map.

The lowest boundary is presented between the data from the undamaged state and damage 2 in the U-matrix surface. If the results of the classification are compared with respect to all the temperatures, it can be concluded that the damages have been correctly classified. Moreover, the way the outliers have been treated does not imply the creation of a new cluster. The undamaged state in all the temperatures is clearly separated from the rest of the damages although the number of output neurons in the cluster map is different for each temperature.

The results in the previous two studies have shown that the proposed methodology applied to data coming from dynamic responses at different temperatures allows a proper final classification in the cluster map and the U-matrix surface. However, these results change from one temperature to another and the distribution at each temperature is different. Therefore, these results suggest that changes in the temperature during the inspection can probably lead to false results in the final classification.

5.1.3. Damage detection and classification using all temperatures. The third study with the aluminum plate is aimed to solve the question about how it is possible to improve the

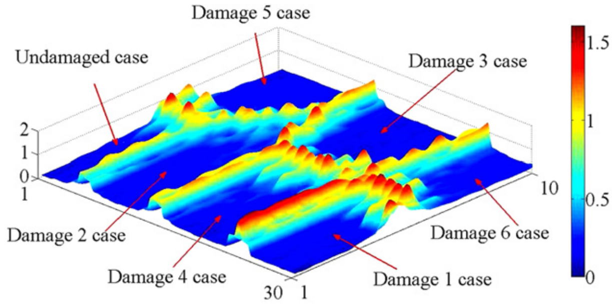

Figure 17. Classification of the different states at 50 °C using 10 scores and the SPE-index using the U-matrix surface.

final classification pattern by considering the data covering different temperature ranges. As a possible solution, in order to improve the robustness of the methodology to temperature changes, the data from the different temperatures are organized and processed as it has been explained in section 4. In the previous cases, we have just used 10 scores. However, the use of data from all the temperatures increases the number of scores that have to be considered. In this case, the optimal set of parameters to configure the map was found to be as follows: 150 scores, normalization HistD, a hexagonal lattice with a flat sheet shape and a cluster size of 30 × 30. In spite of the number of scores being high, the feature vector built with this number of scores and the SPE-index corresponds to a reduced version compared with the use of the raw signals or all the approximation coefficients.

The results are presented in the figures 18 and 19 by means of the cluster map and the U-matrix surface. Results show a clear distinction between the different structural states in both figures. This distinction can be observed by the different data sets with different colours in the cluster map. The main difference with the previous results is that damage 3 is now separated into two groups. This result can also be confirmed by evaluating the U-matrix surface. It is also worth noting the presence of small zones inside of each damage case in the U-matrix surface and the cluster map. In the U-matrix surface, the damage cases are separated by the highest boundaries, the sub-groups are represented by the dark blue colour and the separation between these sub-groups is represented by the light blue colour. More precisely, six sub-cases can be identified for each damage case. These six cases correspond to the data at the six temperatures. These results confirm that the methodology allows a proper identification of the different types of damage despite the changes in the temperature.

5.2. Multi-layered composite plate

The evaluation of the damage detection and classification methodology using this specimen was performed by means of the following three studies:

(a) Damage detection and classification at different temperature levels.
(b) Damage detection and classification of different damages at different temperatures when the baseline is built using the data from all temperatures.

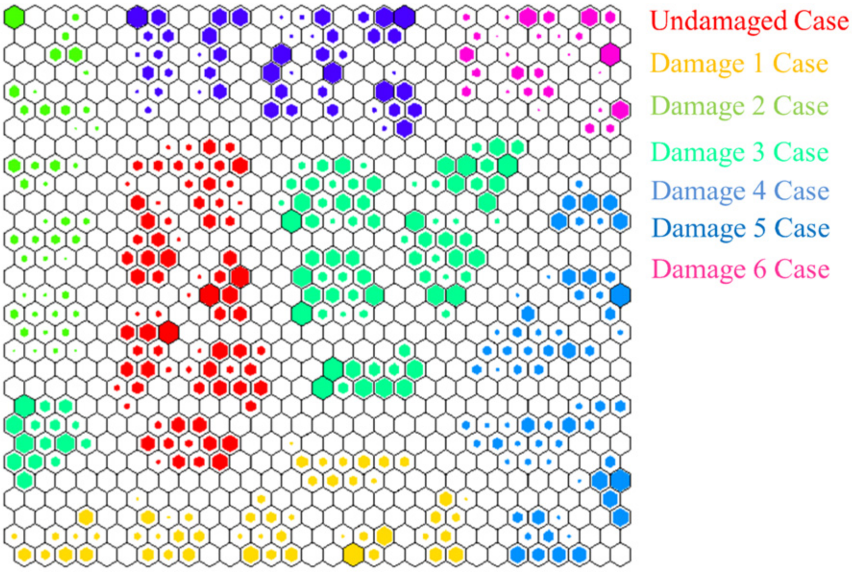

Figure 18. Classification of the different states using all temperatures, 150 scores, SPE-index, normalization type histD and map size 30×30 in the cluster map.

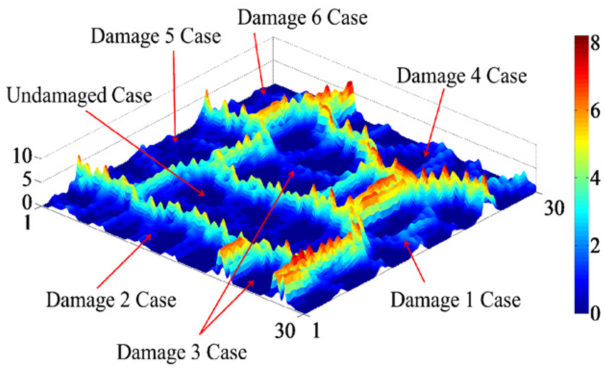

Figure 19. Classification of the different states using all temperatures, 150 scores, SPE-index, normalization type histD and map size 3×30 in the U-matrix surface.

(c) Damage detection and classification of the same damage at different temperatures when the baseline is built using the data from all the temperatures.

To define the optimal set of parameters to configure the map in each study, several SOMs are again trained and validated. As a consequence, a defined number of scores and the SPE-index are used by each actuation phase to define the feature vector. To train the SOM, a normalization type histD is applied to the feature vector, and a hexagonal lattice with a flat sheet shape and a cluster size of 30×10 are used.

5.2.1. Damage detection and classification at different temperatures. Results from the first study are presented in figures 20–25. These figures illustrate the results when the plate is exposed to temperatures of 35, 55 and 75 °C. Similar results are obtained with the rest of the temperatures, but the figures are omitted for space reasons.

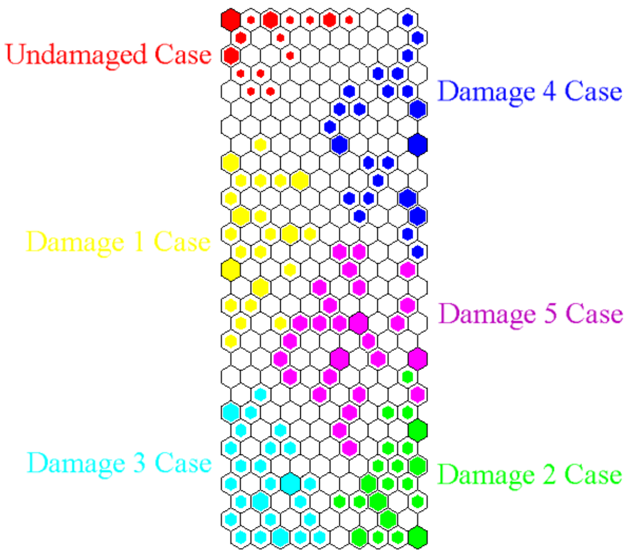

Figure 20. Classification of the different states at 35 °C using five scores and the SPE-index.

Figures 20 and 21 show the results obtained by means of the cluster map and the U-matrix surface at 35 °C respectively. These results show that six structural states are well identified. As it can be shown in the U-matrix surface (figure 21), there is a clear separation between the undamaged state and the rest of damages at this temperature.

Figures 22 and 23 show the results when the multi-layered composite plate is exposed to a temperature of 55 °C. As it has been discussed previously, the cluster map and the U-matrix surface present six well defined clusters. The biggest boundary can also be found between the undamaged state and the rest of damages. However, in this case, the boundary between damage 4 and damage 2 is less evident.

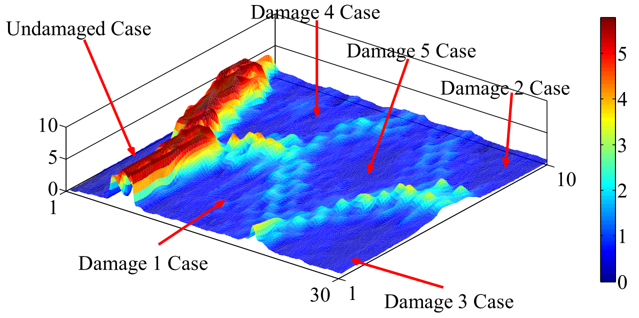

Figure 21. Classification of the different states at 35 °C using five scores and the SPE-index.

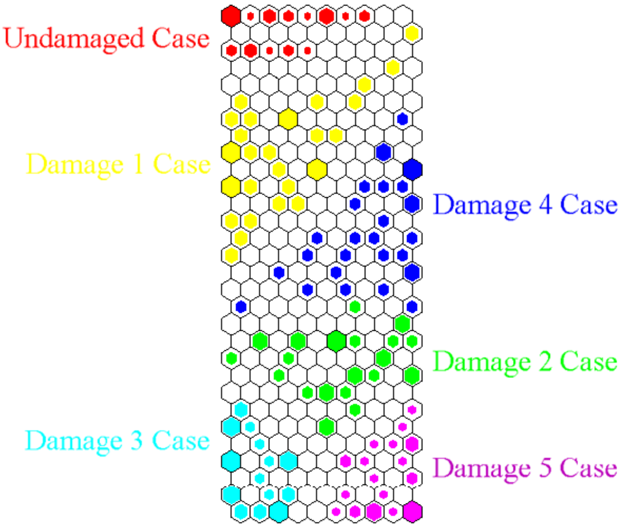

Figure 22. Classification of the different states at 55 °C using nine scores and the SPE-index using the cluster map.

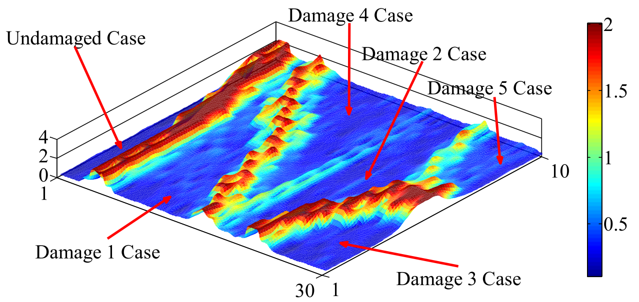

Figure 23. Classification of the different states at 55 °C using nine scores and the SPE-index using the U-matrix surface.

Figures 24 and 25 present the results obtained when the temperature is 75 °C. As well as the previous cases, the undamaged state is clearly separated from the damaged cases.

5.2.2. Damage detection and classification of different damages at different temperatures when the baseline is built using the data from all temperatures. Results from the second study are depicted in figures 26 and 27. In this case, the baseline is built using data from all temperatures. Moreover, five different damages from different temperatures are used. In this respect, damage 1 corresponds to damage 1 when the plate is exposed to a temperature of 35 °C; damage 2 is the damage 2 at 45°;

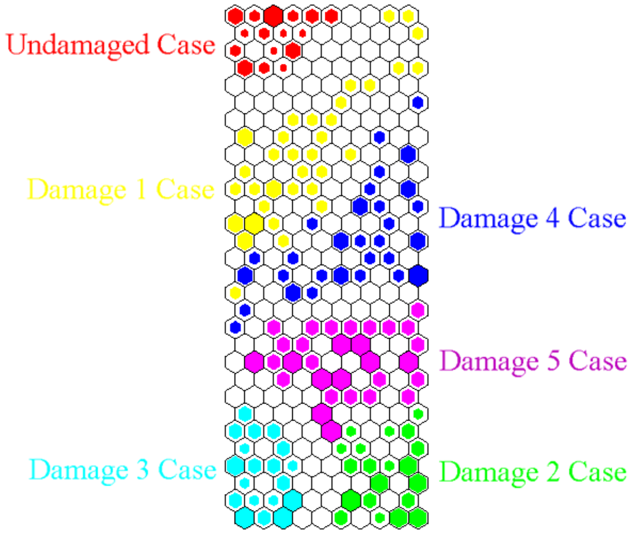

Figure 24. Classification of the different states at 75 °C using 11 scores and the SPE-index in the cluster map.

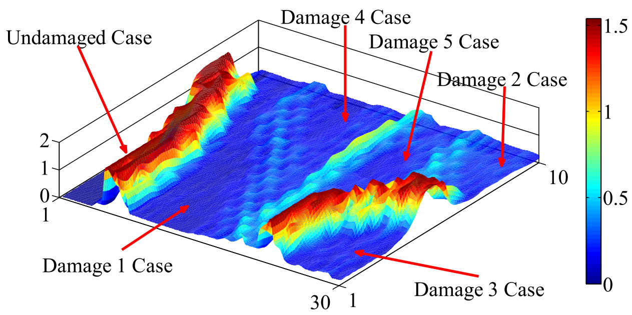

Figure 25. Classification of the different states at 75 °C using 11 scores and the SPE-index in the U-matrix surface.

damage 3 is the damage 3 at 55°; damage 4 is the damage 4 at 65°; and damage 5 is the damage 5 at 75°. The feature vector is formed by 30 scores and the SPE-index of each actuation phase. The observation of the cluster map and the U-matrix surface allows us to identify the different states despite the presence of two outliers (in the undamaged case and in damage 1). In contrast to the previous results, the boundary in the undamaged state is less clear with respect to the rest of boundaries in the U-matrix surface.

5.2.3. Damage detection and classification of the same damage at different temperatures when the baseline is built using the data from all the temperatures. Figures 28 and 29 show the results from the third study. In this case, the baseline is built using the data from all the temperatures. The objective is now to classify the same damage (damage 1) at different temperatures. The feature vector is composed of 30 scores and the SPE-index of each actuation phase. The results in the cluster map and the U-matrix surface show that it is possible to perform the damage detection because there is a clear distinction between the healthy state and the damaged states. Nevertheless, the clusters with damaged states cannot be clearly separated, and some outliers are present in the cluster map. The last remark can be validated using the U-matrix surface since its bound-

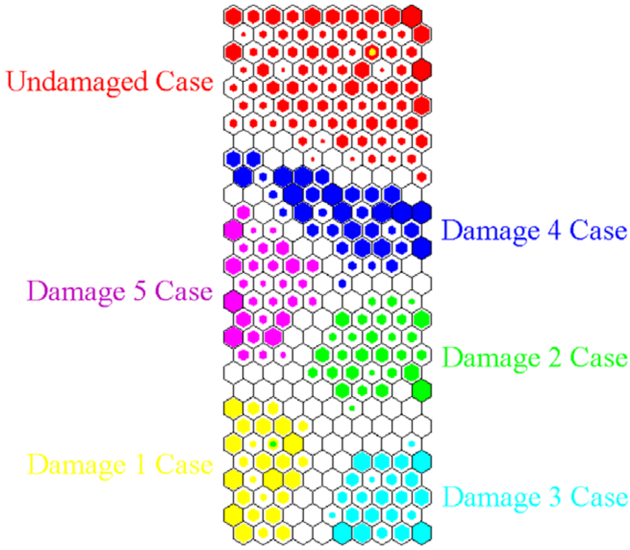

Figure 26. Classification using the baseline with all temperatures and damages at different temperatures and positions.

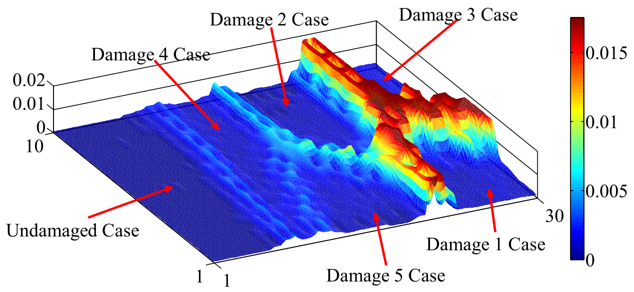

Figure 27. Classification using the baseline with all temperatures and damages at different temperatures and positions.

aries do not have a significant value. As a conclusion, a proper classification of all damages from this case is not possible.

6. Conclusions

An automatic method was proposed for the analysis of ultrasonic signals for the purpose of damage detection and classification under temperature variations. The results obtained showed that there is an influence of the temperature in the variability of the dynamics in the data gathered from the structure when it is subjected to environmental changes in spite of the structural state studied. This result demonstrates that the temperature is an important environmental effect to bear in mind in the design of a SHM system.

The first study indicated that the use of the approach enables one to detect and classify damage in the structure and the breakage at different percentages in the sensor when the data are collected under the same temperature conditions. In the specific cases presented, the pre-processing with DWT, the use of the scores and the SPE-index by each phase and the data fusion by means of a self-organizing map presented the best result in the detection and classification in both structures.

The use of robust baselines as presented in this paper allowed the damage detection in all the cases in spite of temperature changes, and the complexity and type of material

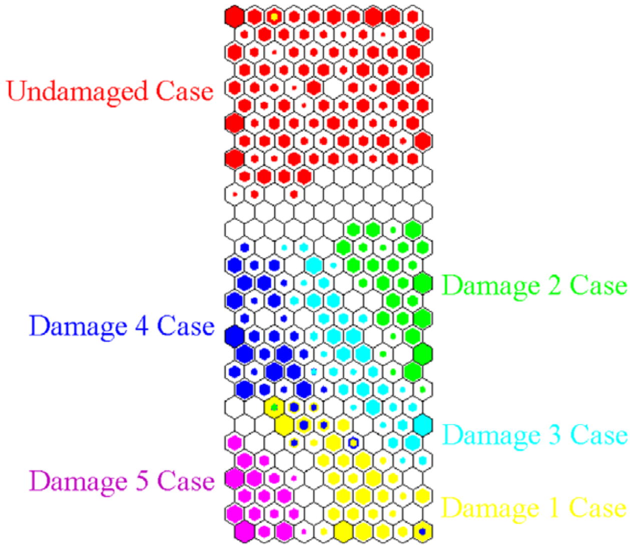

Figure 28. Classification using the baseline with all temperatures and damage 1 as damage at all temperatures in the cluster map.

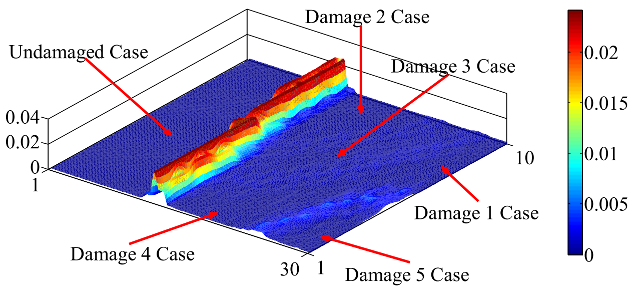

Figure 29. Classification using the baseline with all temperatures and damage 1 as damage at all temperatures in the U-matrix surface.

of the evaluated structures. According to the results, in all the evaluated cases there was a clear separation between the healthy state and the damage states in the cluster map and the U-matrix surface.

In the classification problem, the use of robust baselines allowed classification in most of the cases with the exception of the same damage at different temperatures in the simplified aircraft composite skin panel where the use of scores and SPE-index do not allow classification. In this specific case, additional studies need to be performed to obtain a better classification of all the damaged states.

Finally, it is necessary to highlight that with the application of this approach, the problem of evaluating all the phases to define the existence of damage especially in large structures instrumented with several PZT transducers is solved. The solution implies only the evaluation of the cluster map or the U-matrix surface obtained by data fusion.

Acknowledgments

The authors would like to express their gratitude to the Research School on Multi Modal Sensor Systems for Environmental Exploration (MOSES) and the Centre for Sensor Systems (ZESS) for sponsoring the research presented herein. The authors would like further to acknowledge support from the Education Ministry in Spain through 'Movilidad de estudiantes en programas de doctorado con mención hacia la excelencia' which supported Maribel Anaya and Diego Tibaduiza's placement in Siegen and to the 'Ministerio de Ciencia e Innovación' in Spain through the coordinated project DPI2011-28033-C03-01. Finally, the authors thank Mr Gerhard Dietrich, Ms Inka Buethe and Mr R Singh from the University of Siegen for their support during the execution of the experimental phase.

References

[1] Rytter A 1993 Vibration based inspection of Civil Engineering Structures *PhD Thesis* Aalborg University Denmark

[2] Overly T, Park G, Farinholt K and Farrar C 2009 Piezoelectric active-sensor diagnostics and validation using instantaneous baseline data *IEEE Sensor J.* **9** 1414–21

[3] Tibaduiza D A 2013 Design and validation of a structural health monitoring system for aeronautical structures *PhD Thesis* Universitat Politècnica de Catalunya

[4] Sohn H 2007 Effects of environmental and operational variability on structural health monitoring *Phil. Trans. R. Soc.* A **365** 539–60

[5] Dodson J C and Inman D J 2013 Thermal sensitivity of Lamb waves for structural health monitoring applications *Ultrasonics* **53** 677–85

[6] Jolliffe I T 2002 *Principal Component Analysis (Springer Series in Statistics)* (Berlin: Springer)

[7] Mujica L E, Rodellar J, Fernandez A and Güemes A 2011 Q-statistic and T^2-statistic PCA based measures for damage assessment in structures *Struct. Health Monitoring* **10** 539–53

[8] Alcala C F and Qin S J 2009 Unified analysis of diagnosis methods for process monitoring *Proc. 7th IFAC Symp. Fault Detection, Supervision and Safety of Technical Process (Barcelona)* pp 1007–12

[9] Li G, Qin S J, Ji Y and Zhou D 2009 Reconstruction based fault prognosis for continuous processes *Proc. 7th IFAC Symp. on Fault Detection, Supervision and Safety of Technical Process (Barcelona)* pp 1019–24

[10] Tibaduiza D A, Mujica L E and Rodellar J 2011 Comparison of several methods for damage localization using indices and contributions based on PCA *J. Phys.: Conf. Ser.* **305** 012013

[11] Kohonen T 1990 The self-organizing maps *Proc. IEEE* **78** 1464–80

[12] Torres Arredondo M A, Buethe I, Tibaduiza D A, Rodellar J and Fritzen C-P 2012 Damage detection and classification in pipework using acousto-ultrasonics and probabilistic non-linear modelling *CSHM-4: Civil Structural Health Monitoring Workshop* (on CD-ROM)

[13] Kohonen T and Honkela T 2007 Kohonen network *Scholarpedia* **2** 1568 (http://www.scholarpedia.org/article/Kohonen_network)

[14] Worden K, Staszewski W J and Hensman J J 2011 Natural computing for mechanical systems research: a tutorial overview *Mech. Syst. Signal Process.* **25** 4–111

[15] Mallat S G 1989 A theory for multiresolution signal decomposition: the wavelet representation *IEEE Trans. Pattern Analysis Machine Intell.* **11** 674–93

[16] Coifman R R and Wickerhauser M V 1992 Entropy-based algorithms for best basis selection *IEEE Trans. Inform. Theory* **38** 713–8

[17] Mallat S 1997 *A Wavelet Tour of Signal Processing* 2 edn (San Diego, CA: Academic) ISBN 0-470-22153-4

[18] Newland D E 1993 *Random Vibration, Spectral and Wavelet Analysis* (New York: Longman, Harlow and John Wiley)

[19] Tibaduiza D A, Mujica L E and Rodellar J 2012 Damage classification in structural health monitoring using principal component analysis and self-organizing maps *Struct. Control Health Monit* **20** 1303–16

[20] Wold S, Geladi P, Esbensen K and Ohman J 1987 Multiway principal component and PLS analysis *J. Chemomet.* **1** 41–56

[21] Nomikos P and MacGregor J F 1994 Monitoring batch processes using multiway principal component analysis *AIChE J.* **40** 1361–75

[22] Westerhuis J, Kourti T and MacGregor J 1999 Comparing alternative approaches for multivariate statistical analysis of batch process data *J. Chemomet.* **13** 397–413

[23] Kalogiannakis G and Hemelrijck D V 2011 Classification of wavelet decomposed AE signals based on parameter-less self-organized mapping *Int. J. Mater. Prod. Technol.* **41** 89–104

[24] Taha M M R, Noureldin A, Lucero J L and Baca T J 2006 Wavelet transform for structural health monitoring: a compendium of uses and features *Struct. Health Monitoring* **5** 267–95

[25] Vesanto J, Himberg J, Alhoniemi E and Parhankangas J 2000 *SOM Toolbox for Matlab 5* (Helsinki: Helsinki University of Technology)

[26] Ruiz M, Sin G, Berjaga X, Colprim J, Puig S and Colomer J 2011 Multivariate principal component analysis and case-based reasoning for monitoring, fault detection and diagnosis in a WWTP *Water Sci. Technol.* **64** 1661–7

[27] Cherry G and Qin S J 2006 Multiblock principal component analysis based on a combined index for semiconductors fault detection and diagnosis *IEEE Trans. Semicond. Manufact.* **19**

[28] Pachghare V K, Kulkarni P and Nikam D M 2009 Intrusion detection system using self organizing maps *IAMA 2009: Int. Conf. Int. Agent Multi-Agent Syst.* doi:10.1109/IAMA.2009.5228074

[29] Walter J A and Schulten K J 1993 Implementation of self-organizing neural networks for visuo-motor control of an industrial robot *IEEE Trans. Neural Netw.* **4** 86–96

[30] Kasabov N, Nikovski D and Peev E 1993 Speech recognition based on Kohonen self-organizing feature maps and hybrid connectionist systems *Proc. First New Zealand International Two-Stream Conf. on Artificial Neural Networks and Expert Systems* doi:10.1109/ANNES.1993.323068

[31] Ghimire B, Sinanovic S, Haas H and Auer G 2009 Self-organised interference mitigation in wireless networks using busy bursts *ISABEL 2009: 2nd Int. Symp. on Applied Sciences in Biomedical and Communication Technologies*

[32] Vesanto J and Alhoniemi E 2000 Clustering of the self-organizing map *IEEE Trans. Neural Netw.* **11** 586–600

[33] Tibaduiza D A, Mujica L E and Rodellar J 2013 Damage classification in structural health monitoring using principal component analysis and self-organizing maps **20** 1303–16

[34] Torres Arredondo M A, Tibaduiza D-A, Mujica L E, Rodellar J and Fritzen C-P 2012 Damage assessment in a stiffened composite panel using non-linear data-driven modelling and ultrasonic guided waves. *Proc. 4th Int. Symp. on NDT in Aerospace (Augsburg)* (on CD-ROM)

[35] Clarke T, Simonetti F and Cawley P 2010 Guided wave health monitoring of complex structures by sparse array systems: influence of temperature changes on performance *J. Sound Vibr.* **329** 2306–22

[36] Dodson J C and Inman D J 2013 Thermal sensitivity of Lamb waves for structural health monitoring applications *Ultrasonics* **53** 677–85

[37] Lu Y and Michaels J E 2005 A methodology for structural health monitoring with diffuse ultrasonic waves in the presence of temperature variations *Ultrasonic* **43** 717–31

[38] Park G, Farrar C R, di Scalea F L and Coccia S 2006 Performance assessment and validation of piezoelectric active-sensors in structural health monitoring *Smart Mater. Struct.* **15** 1673–83